# The Vortex Lattice of a Type II Superconductors Studied by Small Angle Neutron Scattering

*Author:*
Dr. J. L. GAVILANO

**PAUL SCHERRER INSTITUT**

2015

**Abstract**

In this laboratory work we will study the vortex lattice VL of a type II superconductor using Small Angle Neutron Scattering SANS. The sample is a single crystal of Nb, a superconductor with a $T_c = 9.3$ K and lower and upper critical fields of $\mu_0 H_{c1} = 0.18$T and $\mu_0 H_{c2} = 0.4$T, respectively. For external magnetic fields between $H_{c1}$ and $H_{c2}$ the superconductor is in the so-called intermediate state. There, the magnetic field partially penetrates the material in the form of individual flux lines, forming a regular lattice, the "vortex lattice" VL. This lattice can be directly probed using small angle neutron scattering SANS techniques. In this experiment we will study the behaviour of the VL as a function of the magnetic field.

# 1 Introduction

## 1.1 Superconductivity

A superconductor is a material that (i) conducts electrical current with no resistance ("perfect conductivity") and (ii) expels magnetic fields from its interior ("Meissner effect"). Superconductivity was first discovered in Hg by the Dutch physicist Heike Kamerlingh Onnes in 1911 in Leiden. In the superconducting state no heat, sound or any other form of energy would be released from the material below the "critical temperature" $T_c$, i.e., the temperature at which the material becomes superconducting. The transition normal-superconducting is abrupt, a phase transition. See Figure 1.1. However, for most materials this occurs only at extremely low temperatures.

There are two classes of superconductor, type-I and type-II, based on their behaviour under an applied magnetic field. Figure 1.2 shows the ideal bulk magnetisation curves for both types, and the intrinsically different behaviour. In type-I superconductors the magnetisation curve is characterised by the full Meissner effect. This means an almost complete expulsion of internal fields from the bulk of the superconductor, barring a surface depth of characteristic dimension $\lambda_L$, the London penetration depth. As $B = \mu_0(M+H)$, and $B = 0$ inside the bulk, the magnetisation follows $M = -H$. On increasing the field above a critical value $H_c$, the system undergoes a first-order transition into the normal state.
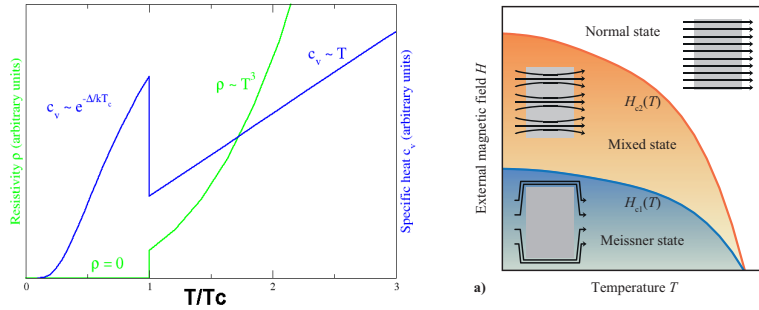
Figure 1: Phase transition normal - superconducting state and (right) Meissner and mixed states of a type II superconductor
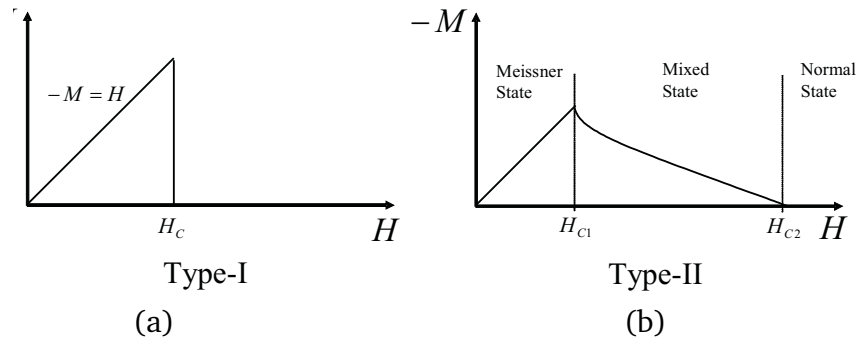


Figure 2: Classes of Superconductors. Below a critical field $H_c$ the Meissner effect is complete in a type I superconductor. In a type II above a critical field the field penetrate in the form of individual lines.

## 1.2 The Vortex Lattice

Magnetic flux can penetrate a type II superconductor in the form of Abrikosov vortices (also called flux lines) each carrying a quantum of magnetic flux $\phi_0 = h/(2e) = 2.068 \times 10^{-15}$ T· m$^2$. These tiny vortices of super current tend to arrange themselves in a triangular flux line lattice VL also called vortex lattice VL, and which is perturbed by material inhomogeneities that pin the flux lines. Many properties of the VL are well described by the phenomenological Ginzburg-Landau theory or by the electromagnetic London theory, which treats the vortex cores as singularities. In Nb the VL is rather

"soft". Thermal fluctuations and random pining oppose to the (ordering) vortex-vortex interaction and may result in a "melting" the VL.

The flux lines in a superconductor are quasi one-dimensional objects: they align along the direction of the magnetic field and are arranged parallel to each other and forming a triangular lattice in a plane perpendicular to the external field. Flux quantisation dictates that the minimum distance $d$ between lines of flux lines is given by

$$d = \sqrt{\frac{\sigma \phi_0}{H}}, \tag{1}$$

where $H$ is the applied field, $\phi_0$ is the flux quantum and $\sigma$ is a dimensional constant that depends on the VL structure. $\sigma = 1$ for a square lattice, and $\sigma = \sqrt{3}/2$ for an hexagonal lattice.

Table 1: Distance between nearest neighbours planes of flux lines in a VL in Nb

| H in T | d in Å |
|--------|--------|
| 0.2 | 946 |
| 0.3 | 772 |
| 0.4 | 669 |

# 2 Neutron Scattering

The most prominent scattering techniques in material research use photons, electrons or neutrons. Owing to the different properties of the scattered particle, regarding charge, spin, mass and energy, one often selects a combination of the complementary scattering techniques to obtain a complete view on the investigated problem.

The neutron was discovered in 1932 and four years laters it was found that it can Bragg diffracted by solids. The properties of the neutron are very suitable for condensed matter research: it is electrically neutral and has a spin S = 1/2. Neutrons are Fermions and obey Fermi-Dirac statistics. Being uncharged allows neutrons to easily penetrate the bulk of the investigated material and also the experimental equipment, e.g., cryostats, magnets or

pressure cells. This advantage has also a downside: the weak interaction between the neutrons and the nuclei of the scatterer material leads to a low occurrence of scattering events. Therefore, high incident neutron fluxes and long counting times are unavoidable, for example compared to x-ray scattering.

Table 2: Physical Properties of the neutron

| | |
|---|---|
| mass $m_n$ | $1.674110^{-27}$ Kg |
| charge | 0 |
| spin | 1/2 |
| magnetic dipole moment $\mu$ | $-1.913\mu_N$ |
| free neutron life time $\tau$ | 881.5 s |
| de Broglie wavelength $\lambda$ | $\frac{h}{m_n v}$ |
| kinetic energy E | $\frac{m_n v^2}{2} = \frac{m_n}{2}\left(\frac{h}{\lambda}\right)^2$ |

Neutrons are produced by fission in nuclear reactors or spallation at accelerator-based sources and then moderated to the required energy. They are then directed to the instruments in neutron guides, using total reflections from "supermirrors" (a neutron supermirror consists of typically 100 highly reflective double layers of Ni/Ti ). The energy of neutrons with a wave-length in the order of interatomic distances matches very well the typical energies of lattice and spin excitations in solids. Therefore, neutron scattering is particularly suitable for investigations of dynamic processes in condensed matter. The second characteristic of the neutron, namely its spin, permits to couple directly the magnetic moments of the bulk material and infer the static as well as dynamic microscopic magnetic properties, such as magnetic structures or excitations.

## 2.1   Neutron Sources

The neutrons used in scattering experiments can be obtained from a nuclear reactor, like the high flux reactors at Oak Ridge National Laboratory ORNL (http://www.ornl.gov/) at Oak Ridge Tennessee and at the Institute Laue-Langevin ILL (http://www.ill.eu/) in Grenoble , The reactor FRMII in Garching near Munich (Germany) or in Saclay near Paris (France). Here the neutrons are produced by spontaneous fusion of $^{235}$U. There are also spalla-

Table 3: Wavelength, frequency, velocity, and energy relationship for neutrons

| Quantity | Relationship | Value at 2 meV |
|---|---|---|
| Energy | $[meV] = 2.072k^2[\mathring{A}^{-1}]$ | 2 meV |
| Wavelength | $\lambda[\mathring{A}] = \frac{9.044}{\sqrt{(E[meV])}}$ | 6.4 $[\mathring{A}]$ |
| Wave vector | $k[\mathring{A}^{-1}] = \frac{2\pi}{\lambda[\mathring{A}]}$ | 0.982 $\mathring{A}^{-1}$ |
| Frequency | $\nu[THz] = 0.2418E[meV]$ | 0.484 THz |
| Wavenumber | $\nu[cm^{-1}] = \nu[Hz]/(2.998 10^{10}cm/s)$ | 16.1 $cm^{-1}$ |
| Velocity | $v[Km/s] = 0.632k[\mathring{A}^{-1}]$ | 0.62 Km/s |
| Temperature | $T[K] = 11.605E[meV]$ | 23.2 K |

tion sources like SINQ at PSI , where neutrons are produced by bombarding heavy nuclei (like U, W, Ta, Pb or Hg) with high-energy protons.

Thermal neutrons with a Maxwellian energy spectrum around 320 K ($\lambda \sim$ 1.7 Å) and, cooled with moderators at temperatures in the range from 20 K to 40 K are used to generate neutrons with a Maxwellian spectrum around $\lambda \sim 6$ Å. Research reactors work in the same way as nuclear power stations but are designed to yield a high neutron flux leaving the moderator system.

Neutron spallation sources use a beam of accelerated protons to bring the nuclei in a target to an excited state, such that neutrons 'evaporate 'from the target. These neutrons are moderated in the same way as in a reactor to obtain a thermal or cold spectrum of neutrons for scattering experiments. Most spallation sources are pulsed sources, delivering intense pulses of neutron radiation. The Swiss spallation source, SINQ, at Paul Scherrer Institute is an exception from this. Other spallation sources are ISIS near Oxford, UK, or the Spallation Neutron Source, Oakridge National Laboratory, USA. A new European spallation source is being built in Lund, Sweden. It will become operational in 2018 and will be the new European high intensity neutron source.

## 2.2 Reciprocal space and scattering diagram

The laws of momentum and energy conservation governing all diffraction and scatternig experiments are:

$$
\begin{aligned}
\mathbf{Q} &= \mathbf{k_f} - \mathbf{k_i}, \\
|\mathbf{Q}| &= \mathbf{k_i^2} + \mathbf{k_f^2} - 2|\mathbf{k_i}||\mathbf{k_f}|cos(\theta_s), \\
\hbar\omega &= E_i - E_f
\end{aligned}
$$

In these equations, the wave vector magnitude is $k = 2\pi/\lambda$, where $\lambda$ is the neutron wavelength and the momentum transfer to the crystal is $\hbar\mathbf{Q}$. The subscript $i$ refers to the incident beam and $f$ to the diffracted or final beam. The angle between the incident and final beams is $2\theta_s$ and the energy transferred to the sample is $\hbar\omega$. Because of the final mass of the neutron its dispersion relation is

$$
\begin{aligned}
E &= \frac{\hbar^2 k^2}{2m_n} \\
E[meV] &= 2.072 k^2 [\mathring{A}^{-1}] \\
\hbar\omega &= \frac{\hbar^2 k^2}{2m_n}(ki^2 - k_f^2)
\end{aligned}
$$

In any scattering experiment one measures the incident ($i$) and and final ($f$) neutron beams and infers the energy and momentum transferred to the sample. Elastic scattering occurs for $k_i = k_f$. But to understand the process it is necessary to consider the reciprocal lattice of the solid. The dots in the next figure represent the reciprocal lattice for a two-dimensional crystalline solid and each point corresponds to a reciprocal lattice vector. We plot a circle with radius $k$ with centre at the origin of the reciprocal lattice and if it passes through two points of the reciprocal lattice the Bragg condition is satisfied. The circle is called the Ewald circle in two dimensions and Ewald sphere in three dimensions.

In the case of neutron diffraction on a VL, as before, we construct the Ewald sphere (grey) with the incoming wave vector $\mathbf{k}$ parallel to the external magnetic field orientation. The two dimensional reciprocal flux line lattice (VL) appearing in the plane perpendicular to the field is represented as blue spots. In this configuration the sphere touches the reciprocal lattice at only one point. Therefore, the quasi momentum conservation is not satisfied for
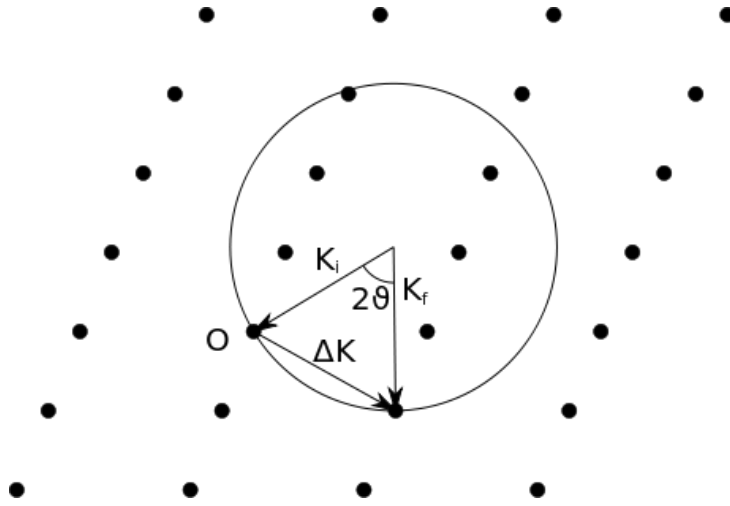
6

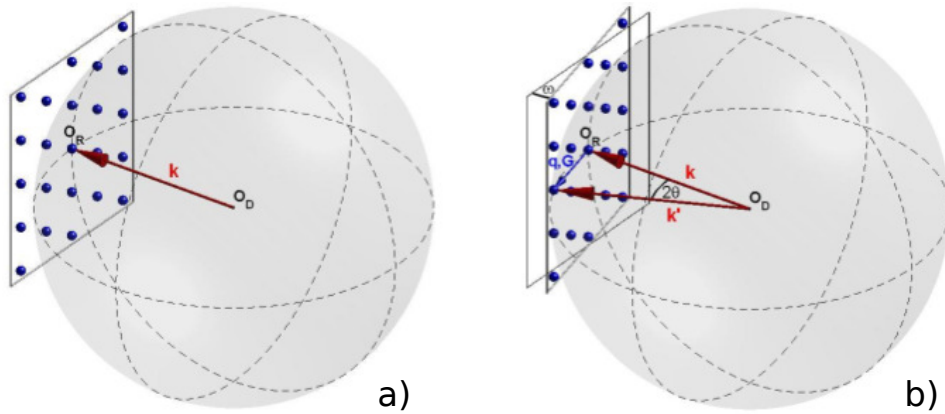Figure 3: Neutron diffraction diagram using Ewald sphere construction.



Figure 4: Ewald Sphere for neutron diffraction of a VL at two at two rocking angles

diffraction to any other point. No Bragg peaks are observed in the detector. b) One rotates the reciprocal lattice by an angle of $\omega$, such that the Ewald sphere touches two points of the reciprocal lattice, then the momentum conservation is satisfied and a Bragg spot is registered in the detector. The angle between **k** and **k'** is given by $2\theta$, which is of the order of 1 degree. Actually the detector is fixed in space and we rotate the sample and magnet by a small

angle, i.e., we scan for Bragg spots by rocking scans. We detect scattering at angles less than 3 degrees and, therefore, the denotation of small angle scattering. This cannot be detected with a conventional neutron diffraction spectrometers that usually detect angles larger than 10 degrees.

## 2.3   Scattering from the vortex lattice

Neutrons interact with with the flux lines via the dipole potential of the neutron magnetic moment within a magnetic field $\mathbf{B}\,(\mathbf{r})$. The scattering potential can be given by

$$V = -\gamma\mu_N\mathbf{B}(\mathbf{r}) \tag{2}$$

where $\gamma = 1.91$, a dimensionless constant, $\mu_N$ is the nuclear magneton and $\mathbf{B}\,(\mathbf{r})$ is the field distribution of the VL. For parallel fields everywhere B = (0, 0, B), as is expected for the ideal VL, the elastic differential cross-section for magnetic scattering becomes

$$\frac{d\sigma}{d\Omega} = \left(\frac{m_n}{2\pi\hbar^2}\right)^2\gamma^2\mu_N^2|\int B(\mathbf{r})exp(i\mathbf{q}\cdot\mathbf{r})d\mathbf{r}|^2 S(\mathbf{q}) \tag{3}$$

Above $\mathbf{q_{h,k}}$ is a vector in the reciprocal lattice. The final result for the integrated Bragg intensity $I(\mathbf{q_{h,k}})$ of a Bragg spot of order $h, k$ can be written as:

$$I(\mathbf{q_{h,k}}) = 2\pi V\phi_n\left(\frac{\gamma}{4}\right)^2\frac{\lambda_n^2}{\phi_0^2 q_{h,k}cos(\zeta)}|F(\mathbf{q_{h,k}})|^2 \tag{4}$$

where $\phi_n$ is the neutron flux per unit area, V is the illuminated volume of the sample, $\lambda_n$ is the neutron wavelength and $cos(\zeta)$ is the Lorentz-factor. The angle $\zeta$ is that which lies between the reciprocal lattice vector and the direction normal to the rotation axis. $F(\mathbf{q_{h,k}})$ is the VL form factor, defined as the two- dimensional Fourier transform of the field-distribution for the VL unit cell.

## 2.4   A rocking-curve measurement

As in any diffraction experiment, the key information obtained from SANS measurements on the VL is obtained by carrying out rocking curve measurements. For the SANS measurements reported in this thesis, this involves

rotating a reciprocal lattice vector through the Bragg condition at the detector, and recording the diffracted intensity as a function of rotation angle. To do this involves careful alignment of the sample with respect to the field and neutron beam, and then rotation of the reciprocal lattice.

To perform a rocking curve measurement, the experimenter chooses a series of angles about which to rotate the reciprocal lattice and measure the diffracted intensity, which typically has the expected Bragg angle at the midpoint. Ideally the angular range should take into account the anticipated angular width of the rocking curve as might be expected from resolution considerations, and be wide enough so that at the widest scanned angles the observed intensity falls to the background level.

In SANS experiments, there are two complementary activities that are carried out on recording the rocking curve of a Bragg spot. The first is to perform background measurements with no VL established in the sample (above $T_c(H)$, or after zero-field cooling). These are then subtracted from foreground measurements where the VL is present, leaving just the diffracted signal from the VL.

From the magnetic field dependence of of the form factor of the VL one can extract the superconducting parameters: the London penetration depth $\lambda_L$ and and the Ginzburg coherence length $\psi$ using a London model that takes into account the finite size of the vortex cores. From the magnetic form factor one may obtain superconducting properties of Nb, $\lambda_L$ and $\psi$ as follows:

$$F(\mathbf{q_{h,k}}) = \frac{Be^{-0.44q^2\psi^2}}{1 + q_{h,k}^2\lambda_L^2} \tag{5}$$

Here B is the applied magnetic field (actually magnetic induction) and $q_{h,k}$ is the field dependent reciprocal lattice vector.

# 3   SANS Spectrometer

A classical SANS instrument has a pinhole geometry, as shown in Fig. 1. A poly-chromatic, 'white'neutron beam is guided to the instrument from the neutron source, and a monochromatic beam is generated by selecting a narrow range of wavelengths with a mechanical neutron velocity selector. Typically, the FWHM of the wavelength distribution of the monochromatic beam is 10% of its peak position. The beam is then collimated using pinholes placed in the collimation section of the instrument before the beam

hits the sample. Scattered neutrons are counted with an area sensitive detector located at some variable distance from the sample. Usually, the flight path from sample to detector has the same length as the collimation section, as this configuration gives the optimal compromise for beam intensity and resolution. A typical SANS detector is a $^3$He detector with an area $\sim 1$ m$^2$ and $128 \times 128$ pixels. The spatial resolution of the detector allows to determine the scattering angle $2\theta$ of the counted neutrons and the corresponding momentum transfer $q = (4\pi/\lambda) \cdot sin(2\theta/2)$. The SANS setup outlined above is typical for continuous neutron sources. Modern SANS instruments offer different sample environments for experiments under tailored conditions with e.g., controlled temperature, applied pressure, electric or magnetic fields, or controlled humidity.
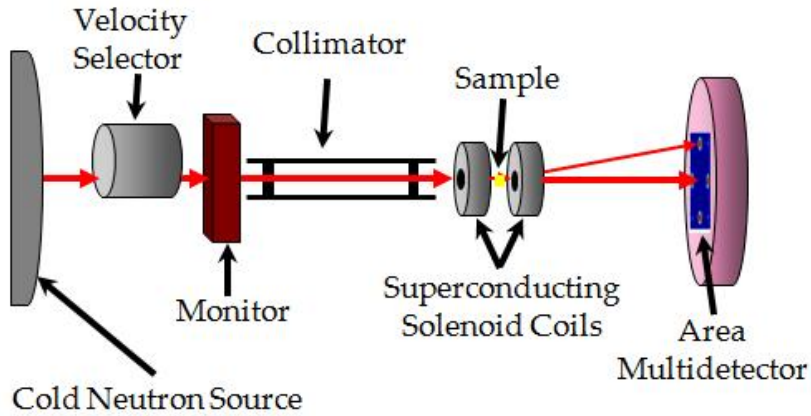


Figure 5: A schematic diagram of a typical SANS instrument. Typically the length of the collimator section is approximately equal to the distance between the sample and the area multidetector, in the traditional pinhole geometry. This distance can be up to 18 m on the SANS-I instrument. Shorter distances are used, especially for larger momentum transfers.

# 4 Data Reduction and Analysis

In order to analyze the signal of the VL, the data measured in the superconducting phase (foreground) were subtracted from the high temperature phase

data (background) for sets at identical conditions of the spectrometer, such as incident neutron wavelengths $\lambda_n$, collimation, detector distance, slits and the same rocking angles. In order to obtain reproducible results, the data were normalized per standard monitor. After every change of wavelength, the beamstop in front of the detector was adjusted to protect the detector from damages caused by the intense direct beam.
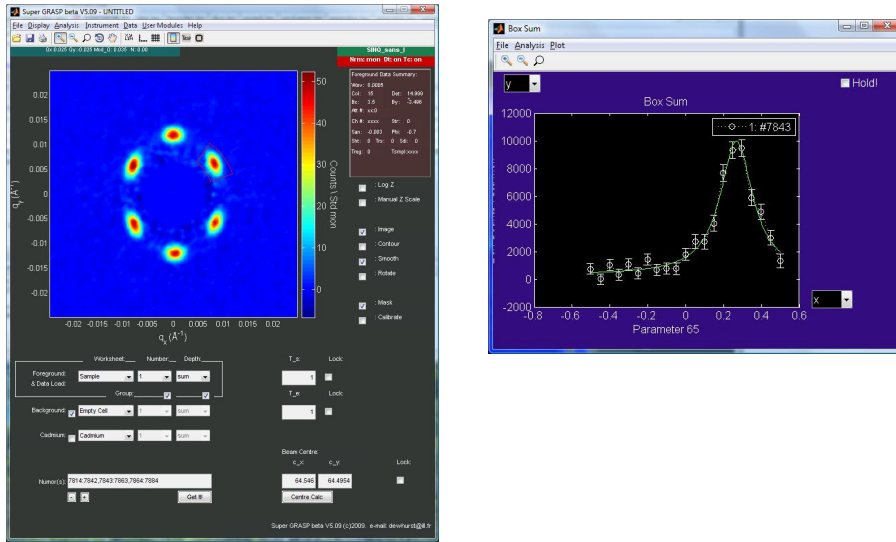


Figure 6: Images of the windows of Grasp. Left main panel where data is loaded for manipulation. Right Image capture of the rocking curve plot output by Grasp and a fit with a suitable line shape functionn

The data manipulation and basic data analysis can be carried out using the GRASP software developed by C.D. Dewhurst at the ILL 18. The software is developed within a Matlab environment, and as such it can handle the two-dimensional and pixelated multidetector data recorded by the SANS instrument. The user interface includes a window that allows a view of the distribution of the diffracted intensity across the multidetector at a certain rotation angle of the reciprocal lattice. It is also possible to sum the measurements at many rotation angles together into just one image, providing a picture of the diffracted intensity over an entire rocking curve. By similarly summing over multiple rocking curves, it is possible to deduce the VL coordination by showing all of the first-order Bragg spots in just one image.

To perform various data manipulations one uses the front panel of Grasp.

One may, for instance, add SANS foreground data summed over numerous rocking curves. The corresponding background data can also be properly subtracted and they are properly normalized. Statistical noise that occurs close to the beam stop can be easily masked. Below we show and Image capture of the front-end of the GRASP software (left). SANS data over multiple rocking curves is loaded, showing all the first-order Bragg spots in a single image. A sector box is defined on the detector over area occupied by the upper right Bragg spot. At the right we show an image capture of a rocking curve plot output by the GRASP software, and fit with a suitable lineshape function. The horizontal axis is in units of degrees of rotation angle of the reciprocal lattice about the vertical axis, where zero corresponds to the straight through position. The vertical axis is in units of total counts within the sector box per standard monitor.

# 5   Experimental Procedure

1. Before the experiment, estimate the vectors ($q_{1,0}$ and $q_{0,1}$) of the reciprocal lattice of Nb (hexagonal lattice) for various applied fields, between 0.2 and 0.4T

2. For the same fields determine the scattering angles $2\theta$ between the incident and final neutron beam for a neutron beam of incident energy of 4 - 5 meV.

3. You will be given a Nb single crystalline sample. Measure its dimensions and mass. The sample will be surrounded by Cd that will determine its area to be illuminated. Cd is a good neutron absorber and in this experiment no neutrons will go through the Cd plate.

4. Mount the Nb sample in a sample holder, insert it into the cryo-magnet (MA11) and start cooling the system.

5. Using the neutron camera verify that the sample is in position (i.e., at the centre of the neutron beam).

6. Adjust the beam stop, intended to block the direct beam to protect the detector.

7. Three different measurements are required for each configuration of the instrument: (a) empty beam or transmission. One has here an attenuated beam and remove the beam stop. This will provide a measure for the neutron flux. (b) background and (c) foreground measurements as described below.

8. Cool the system to 10 K, above $T_c$, where you will perform "rocking scans" as background measurements (measurements in the normal state.

   In a rocking scan one changes stepwise the direction of the magnet with respect to the incident beam. This change results in an optimisation of a Bragg peak (i.e. maximum intensity) for a certain "rocking angle"

9. Apply fields between 0.18 and 0.4T and at each field cool down the sample to the lowest temperature, 1.8 K.

10. Perform foreground measurements (the same scans as in the background measurements, but in the superconducting state).

11. Using Grasp make sets of foreground - background signals. Sum all the data (with the background subtracted) and measure the opening angles between the Bragg spots.

12. Using Grasp make plots of intensity vs. rocking angle. Determine the position and width of the Bragg peaks.

13. At home: from the above data calculate the form factor as a function of applied field.

14. At home (optional): Fit the form factor data to the London model corrected for the finite neutron cores, as explained above and extract the London penetration depth of Nb and the Ginzburg coherence length at the lowest temperature.

More information of the instrument is available in our Web page
http://www.psi.ch/sinq/sansi/sans-i
The description of the program running the experiment, SICS, is described at

http://www.psi.ch/sinq/sansi/manuals.
The description of the program running the sample environment (temperature, fields) Sea

# References

[1] C. G. Windsor. *An introduction to small-angle neutron scattering.* J. Appl. Cryst., 21,582, 1988.

[2] G. L. Squires. *Introduction to the theory of thermal neutron scattering.* Cambridge University Press, Cambridge, 1978.

[3] J. Kohlbrecher and W. Wagner, Appl. Cryst. 33, 804 (2000).

[4] C. D. Dewhurst and R. Cubitt, Physica B 385-386, 176 (2006).

[5] M. Eskildsen et al., Rep. Prog. Phys. 74 124504

[6] D Mazzone et al., Phys. Rev. B **90**, 20507(R), (2014).